Spectroscopic measurements of electron density of capillary plasma based on Stark broadening of hydrogen lines

J. Ashkenazy, R. Kipper, and M. Caner
Soreq Nuclear Research Center, Yavne 70600, Israel
(Received 11 October 1990; revised manuscript received 26 December 1990)

A set of measurements of the electron density of plasma jets, generated by a high-pressure discharge capillary operating at quasi-steady-state, is described. The method of measurement is based on the dependence of Stark broadening of the hydrogen H_α and H_β spectral lines on the electron density. Spectra were sampled electronically, time integrated over the electrical pulse duration, for various capillary currents and at different axial locations along the emerging plasma jet. The comparison of model predictions [Loeb and Kaplan, IEEE Trans. Magn. **25**, 342 (1989)] with electron densities deduced from these spectra, by applying the theory of Stark broadening [Griem, *Spectral Line Broadening by Plasma* (Academic, New York, 1974)], indicates a good agreement over the tested current (1–8 kA) and density (10^{17}–10^{19} cm^{-3}) ranges. At larger densities, self-absorption might be a problem.

I. INTRODUCTION

The high-pressure discharge capillary is a narrow pipe, made of a plastic material (usually polyethylene), placed between two electrodes, one of which is hollow. The two electrodes are connected to a pulse-forming network (PFN). The plasma inside the pipe, generated initially by electrically evaporating a thin metal wire, is heated resistively by the electric current, flowing between the electrodes. This causes radiation to the walls, which in turn induces ablation of the capillary material which is added to the plasma. As a result, a high pressure is developed inside the capillary, causing a mass flow outward through the open electrode. If the electrical pulse duration is long compared to the hydrodynamic time l/c_s, where l is the length of the pipe and c_s is the plasma sound velocity, a quasi-steady-state is reached.

A model for the analysis of the steady-state operation of the discharge capillary was developed by Loeb and Kaplan.[1] In this model, which is summarized in the Appendix, the plasma characteristics are obtained from energy- and mass-conservation considerations. A computer code was written, based on the model, which calculates the discharge parameters for a given capillary geometry (length and radius) and for a given current. The code uses the SESAME equation-of-state[2] library to calculate thermodynamic quantities. Saha equations are incorporated to solve for the average ionization and for the electron density.

In this paper we describe a set of measurements of the electron density of capillary produced plasma jets and compare them with the model predictions. The method of measurement is based on the Stark broadening of spectral lines of atomic hydrogen, which is a constituent of polyethylene plasma. The existence of charged particles in the plasma is associated with a microscopic electric field which interacts with the hydrogen atoms (Stark effect). Due to the statistical nature of this field, it results in broadening of the atomic lines. For the relatively cold and dense plasma, produced by the capillary, the linewidth is dominated by this effect. The Balmer lines H_α (6562.7 Å) and H_β (4861.3 Å) were chosen for observation. The dependence of the linewidth of these transitions on the electron density is described and tabulated in the literature.[3]

The spectrum of the light emitted from the jet, just outside the hollow electrode, is transferred to a digital oscilloscope via a photodiode array, located at the output slit of the spectrograph. Due to speed limitations of the photodiode array, measurements were time integrated over the pulse duration. For the purpose of comparison with theory, they were related to the average (root mean square, rms) current of the pulse.

In Sec. II, the Stark broadening mechanism is shown to be dominant in determining the width of hydrogen lines in our plasma, and the method of deducing the electron density from the linewidth is briefly outlined. In Sec. III, after the experimental setup is described and the method of data processing is explained, results are presented and discussed. They indicate a good agreement with the theoretical predictions of the model over the tested current (1–8 kA rms) and density (10^{17}–10^{19} cm^{-3}) ranges. Self-absorption effects may be a problem at large densities. Measurements of the capillary resistance versus current are shown also.

II. STARK BROADENING OF HYDROGEN LINES

Line broadening in plasma is affected mainly by two physical mechanisms. Doppler broadening occurs as a result of the thermal motion of the radiators relative to the observer. Pressure broadening is caused by the interaction of the radiators with surrounding particles, and, in plasmas, it is dominated by collisions between the radiators and charged perturbers. Since electric fields are involved, it is called Stark broadening.

The Doppler line profile, for radiators at thermal equilibrium, has the shape of a Gaussian distribution with a linewidth $\Delta\lambda_D$ [full width at half maximum (FWHM)] given by[4]

$$\Delta\lambda_D = 2\left[\frac{2kT\ln 2}{Mc^2}\right]^{1/2}\lambda_0 , \quad (1)$$

where λ_0 is the unshifted wavelength and M is the radiator mass. In the case of our capillary hydrogen plasma ($kT \approx 1-2$ eV), the Doppler width of the Balmer H_α (6562.7 Å) and H_β (4861.3 Å) lines is in the range of 0.3–0.7 Å.

Stark broadening results from the interactions of the radiator atom with the electric field, produced by the charged plasma particles at the location of the radiator. Thus it depends on the density of charged particles in the plasma. For singly charged ionized plasma, the electron density N_e is equal to the ion density N_i. Based on the theory of Stark broadening,[3] which takes into account quasistatic ion and impact-electron-broadening effects, the expression for the electron density in terms of the linewidth of hydrogen lines is

$$N_e = 8.02\times 10^{12}\left[\frac{\Delta\lambda_{1/2}}{\alpha_{1/2}}\right]^{3/2} , \quad (2)$$

where $\Delta\lambda_{1/2}$ is the linewidth (FWHM) in angstroms. The reduced wavelength $\alpha_{1/2}$ is a function of the electron density and temperature, i.e., $\alpha_{1/2}=\alpha_{1/2}(N_e,T)$, tabulated in Table III.a. of Ref. 3 for the H_α and H_β lines. In the few cases where the deduced density was below 10^{17} cm^{-3}, ion-dynamical corrections to the $\alpha_{1/2}$ values of H_α were included, using data taken from Ref. 5.

In the set of measurements described in this work the electron density was in the range of $10^{16}-10^{19}$ cm^{-3}. The Stark broadening width (FWHM) corresponding to these densities for H_α and H_β is of the order of 5–300 Å. Therefore the Doppler broadening contribution was neglected.

III. MEASUREMENTS

A. The experimental setup

The experimental setup is shown in Fig. 1. The PFN consists of four sections of 21-μF capacitors and 4-μH inductors. This corresponds to an impedance of 0.44 Ω and a pulse-width of 73 μsec. The capillary is contained in a durable plastic (Delarin) holder, to hold against the high pressure developed during the discharge. Two electrodes, made of a tungsten alloy, are placed on both ends of the capillary. One electrode, connected to the high voltage lead, seals the rear end, while the grounded electrode in front is hollow. An ignitron switch closes the electrical circuit on command. The current pulse is measured by a Rogowski coil, while the voltage pulse is measured by a combination of a shunt resistor and a second Rogowski coil.

The plasma jet is injected through the open electrode into a vacuum vessel ($P \approx 10^{-2}$ Torr). Light emitted from the jet is coupled out via a side window and a focusing lens, both made of quartz, to the entrance slit of a Czerny-Turner 1-m spectrograph (Jarrel-Ash model 78-6400). A 295-groove/mm grating was used in these measurements. It has a specified reciprocal linear dispersion at the exit slit of 32.8 Å/mm. The focal length of the lens and the distances are chosen so that the image of the jet is in the plane of the entrance slit, which was open 40 μm wide. Thus the light from a narrow slice of the jet enters the spectrograph. By moving the focusing lens parallel to the capillary axis, one is able to image slices from different axial locations along the jet, on the entrance slit.

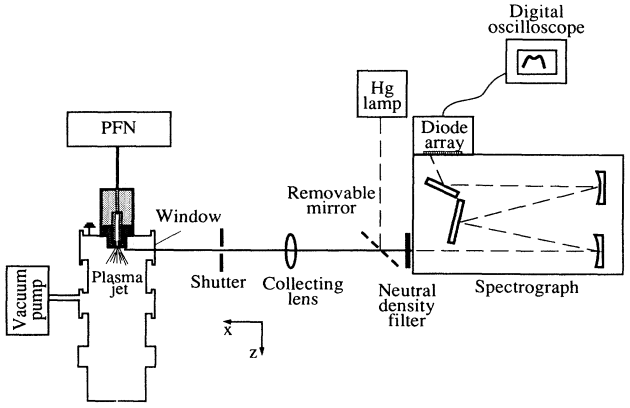

FIG. 1. The experimental setup: Light emitted from the plasma jet is coupled via a quartz lens to the spectrograph. The output spectrum is sampled by the photodiode array and recorded on the digital oscilloscope.

The spectrum on the output slit is sampled by a 1-in.-long, 1024-cell, Hamamatsu linear photodiode array (S2304 series). This is a self-scanning array with 25-μm center-to-center spacing and 2.5-mm-wide cells. The diode array integrates the spectrum with respect to time during the whole discharge. Readout is performed afterward with the help of an external clock. The readout also clears the cells and immediately thereafter a new cycle of integration can begin. With the above-mentioned grating, a spectrum of 833 Å could be sampled simultaneously by the 1-in.-long diode array. A mercury lamp was used for a better calibration of the sampled spectral range (see Fig. 1). The mirror, used to couple its light to the spectrograph, is removed during the capillary discharge. The shutter in front of the collecting lens and the neutral density filter at the entrance slit, shown also in Fig. 1, were used in combination to control the light intensity, in order to avoid saturation of the photodiodes. The spectral response of the photodiode array was measured relative to a calibrated radiometer, using a set of narrow filters in the range 4000–7000 Å. A tungsten lamp was used as the light source in this measurement.

B. Data processing

The sampled spectrum is recorded on a digital oscilloscope (Nicolet 4094C), from which it is transferred to a personal computer for analysis, using the VU-POINT

software package. First, it is divided by the spectral response of the photodiode array. Then, the background is removed and the spectrum is normalized to its maximum.

Figure 2(a) shows a set of four representative H_α spectra taken for different capillary currents. All four spectra were observed 5 mm from the open electrode. They are shown after background subtraction and normalization. Figure 2(b) shows a comparable set of H_β spectra. These spectra demonstrate the Stark broadening of the Balmer lines due to the increase in the electron density as the capillary current is increased. The high wing at the short-wavelength side of the H_β line has to be attributed, most probably, to the tail of the H_γ line.

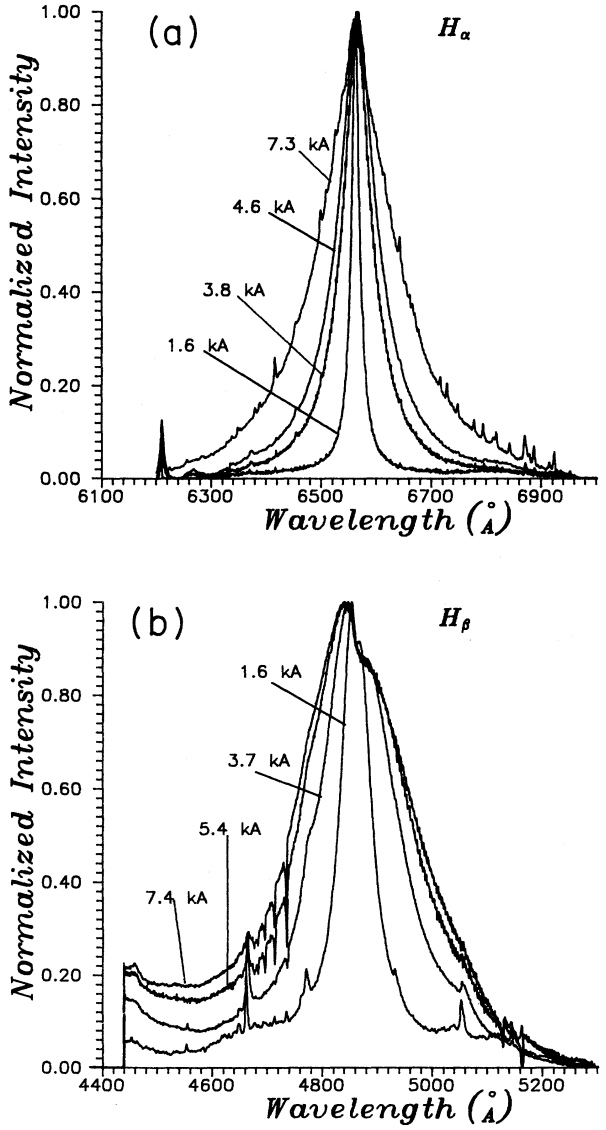

FIG. 2. Representative Balmer spectra each normalized to its maximum, observed 5 mm from the open electrode, for various capillary current values (rms). (a) H_α spectra; (b) H_β spectra.

The linewidth $\Delta\lambda_{1/2}$ (FWHM) is deduced from the normalized spectrum. In order to find the corresponding electron density, Eq. (2) has to be used together with Table AIII.a. in Ref. 3. For this purpose the temperature is calculated from the capillary model[1] (see also the Appendix), which is in fact the theory under test. Nevertheless, this approach seems to be justifiable for the following reasons.

(i) As demonstrated in Fig. 6 (Sec. III D), there is a good agreement between measured and calculated values of the capillary resistance over most of the current range. Since the resistance and temperature of the capillary are closely related,[1] (see also the Appendix), it is an indirect indication that the predicted temperature values are quite good.

(ii) The temperature dependence of $\alpha_{1/2}$ in the relevant range (1–2 eV) is weak, as is obvious from Table AIII.a. in Ref. 3.

To improve the accuracy, a simple interpolation computer program was written. First, for each value of the density in Table AIII.a. in Ref. 3, it interpolates an $\alpha_{1/2}$ value for the specified temperature. Then, interpolating between these values, we get a relation of N_e versus $\alpha_{1/2}$. Together with Eq. (2), which, for the given $\Delta\lambda_{1/2}$, is also a relation of N_e versus $\alpha_{1/2}$, they are solved for N_e (and $\alpha_{1/2}$).

Since the sampled spectrum is a result of time integration over the pulse duration, the obtained electron density has to be regarded as an average value. For the purpose of comparison with theory, it is related to the average (rms) current over the pulse duration.

C. Results and discussion

One type of capillary was used in all the measurements described in this report, having a length $l=5.4$ cm and a radius $a=2.4$ mm. Discharge currents in the range 1–8 kA (rms) were obtained by varying the PFN charging voltage from 1 to 5.5 kV. Spectra were sampled from light emitted from four axial locations along the plasma jet: $z=1$, 3, 5, and 10 mm, where Z is the distance from the edge of the open electrode.

In Fig. 3, electron densities versus current, obtained from H_α and H_β spectra, are compared. Figure 3(a), for which light was sampled at $z=10$ mm, demonstrates a very good agreement between densities obtained from the two Balmer lines. This result can be regarded as a consistency test for our method of measurement. In Fig. 3(b) sampling was done closer to the capillary, at $z=5$ mm, and as a result, measured densities are higher. As can be seen, the consistency between H_α and H_β results holds up to densities of about 5×10^{17} cm^{-3}. Above that, there is a deviation between the H_α and H_β results, which increases with density (discharge current). This fact may not come as a surprise since, as mentioned in the literature,[3] H_β is useful as a density standard for electron densities up to 3×10^{17} cm^{-3}. Thus, for higher densities, only H_α results are presented from now on.

It is important to remember that while the capillary model[1] predicts the value of the electron density inside the capillary, the actual measurement is done outside it.

For that reason, the electron density is measured at more than one location along the jet. Due to the expansion of the emerging jet, the value of the density outside the capillary has to be lower than the corresponding density inside the capillary. However, as the point of observation is moved close to the open electrode, the density is expected to approach the inside value.

Inside the capillary, the plasma is expected to be nearly homogeneous radially, with very sharp gradients near the walls.[1] This behavior, demonstrated experimentally[6] and treated in theory[7,8] for similar discharge devices, is due to the dominant role of radiative transfer in the radial energy transport and its strong dependence on the temperature. This results in a flat temperature profile over most of the cross section, from which follows the transversal homogeneity of other plasma parameters including the density. However, as the jet expands outside the capillary, transversal density variations may become larger. Therefore it is more appropriate to regard the measured electron density at a particular axial location as an average value of the transversal profile of the jet at that axial location. Nevertheless, the reasoning in the preceding paragraph still holds for this average electron density with regard to its relation to the inside value of the electron density.

Figure 4 shows the measured electron density versus current, obtained from H_α spectra, for different axial distances from the capillary. The continuous line represents the model predictions for the electron density inside the capillary. Clearly, it demonstrates the kind of behavior expected above. It is interesting to note that the ratio of the measured density at each axial distance, $z=3$, 5, and 10 mm, to the theoretical value is roughly independent of the current. This may indicate that the shape of the jet is not sensitive to the value of the capillary current. In any case, it is a matter for further investigations.

The measured values of the electron density, just outside the open electrode at $z=1$ mm, are very close to the theoretical values. However, for current above 3 kA (corresponding to $N_e \approx 0.5\times 10^{19}$ cm^{-3}), the measured density becomes larger than theory. This situation is demonstrated more clearly in Fig. 5, where the electron density at $z=1$ mm is compared with theory on a linear scale. As we can see, this discrepancy increases with the current (density).

A possible source of distortions in these measurements is the self-absorption in the plasma which tends to enlarge the linewidth. If the self-absorption contribution to

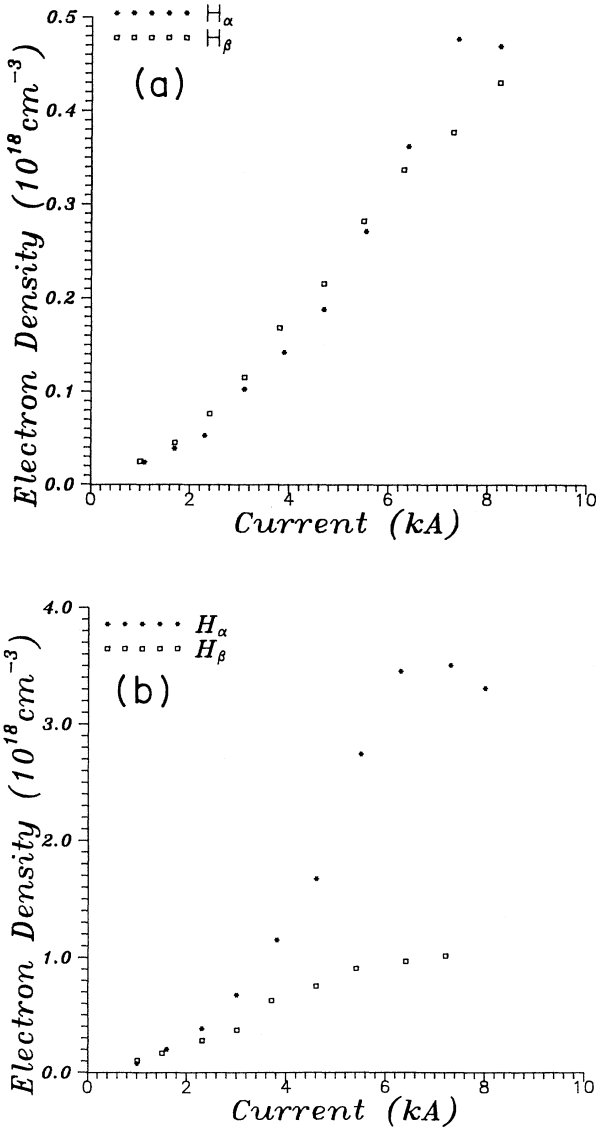

FIG. 3. A comparison between electron densities vs current, obtained from H_α and H_β spectra. (a) Observed 10 mm from the open electrode; (b) observed 5 mm from the open electrode.

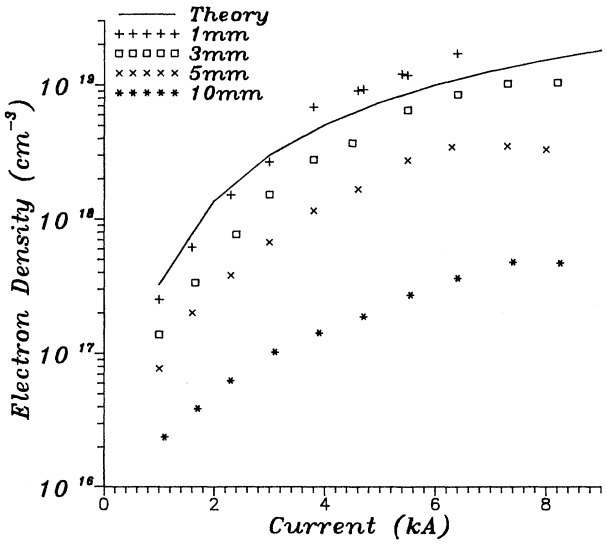

FIG. 4. Electron density vs current, obtained from H_α spectra, observed at different axial distances along the jet from the open electrode: $z=1$, 3, 5, and 10 mm. The continuous line represents the model predictions (Ref. 1) for the electron density *inside* the capillary.

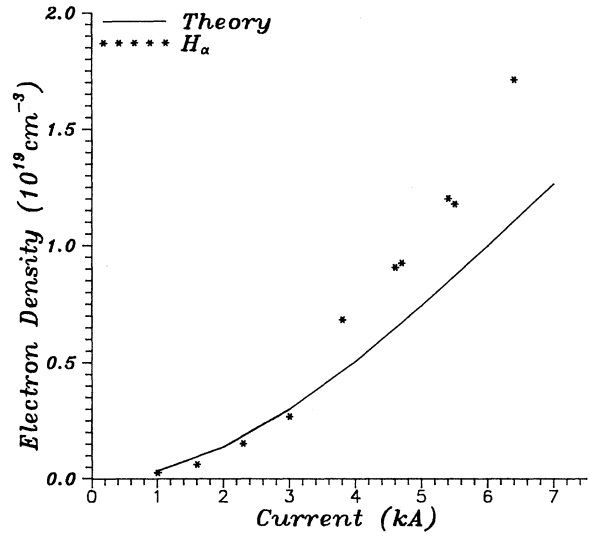

FIG. 5. Electron density vs current, obtained from H_α spectra, observed at an axial distance of 1 mm from the open electrode. The continuous line represents the model predictions (Ref. 1) for the electron density *inside* the capillary.

the width cannot be neglected, then the value of the electron density, derived from the linewidth, would be larger than the actual one. This may be the cause for the behavior demonstrated in Fig. 5, since the absorption coefficient depends on the material density, which is expected to increase with the current. In order to verify this point, the opacity has to be measured. We are now involved in a detailed experimental investigation of the H_α opacity of plasma jets under various conditions and intend to present the results in a subsequent publication.

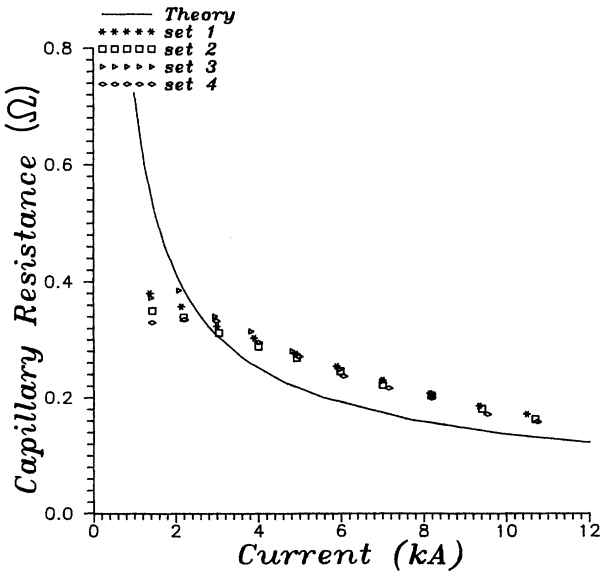

FIG. 6. Measured capillary resistance vs current. The continuous line represents the model predictions (Ref. 1).

D. Capillary resistance

The capillary resistance is deduced from the measured voltage and current pulses. To avoid errors due to parasitic inductances, the resistance is calculated at the current maximum I_{max}, where $dI/dt=0$. We have

$$R(I_{max})=\frac{V[t(I_{max})]}{I_{max}} . \quad (3)$$

In Fig. 6, the measured resistance of our capillary ($l=5.4$ cm, $a=2.4$ mm), versus the current, is compared with theory. The four sets of measurements which are presented demonstrate a good reproducibility. As can be seen, the measured values are somewhat higher than predictions over most of the current range. This may be attributed to electrode and/or line resistance, which are not taken into account by the theory.

IV. CONCLUSIONS

A set of measurements of the electron density of discharge capillary plasma was presented. It is based on the Stark broadening of hydrogen Balmer lines. H_α and H_β spectra were sampled electronically, time integrated over the electrical pulse, for various currents (1–8 kA rms) and at different axial distances from the capillary (1–10 mm). The theory of Stark broadening[3] was then applied to deduce the electron density from these spectra. Results, which were very reproducible, indicate a good agreement with the capillary model[1] over the tested current and density (10^{17}–10^{19} cm^{-3}) ranges. However, measurements at the large density region may have been distorted by self-absorption effects.

In order to extend the measurements to higher densities, the problem of self-absorption has to be verified, and maybe other spectral lines will have to be used. By using a combination of a precision positioner and a narrow entrance slit, the Stark broadening method can be used also to measure the transversal variations of the electron density of the jet. Alternatively, a two-dimensional array could be used. In addition, by using a gated image intensifier between the exit slit of the spectrograph and the sampling photodiode array, time-resolved spectra can be recorded. Thus uncertainties related to the averaging over the pulse duration would be removed.

ACKNOWLEDGMENTS

The authors wish to thank G. Applebaum for his technical assistance. We thank also Professor S. Goldsmith, Professor Y. Maron, Dr. E. Sarid, and Dr. Z. Kaplan for helpful discussions.

APPENDIX

We summarize here the model for the analysis of the quasi-steady-state operation of the discharge capillary, which is described in detail in Ref. 1. This model has been coded into a computational tool which enables the calculation of the various plasma properties for a given capillary length, radius, and discharge current.

A quasi-steady-state is defined by the condition that the variation in the discharge parameters is slow compared with the hydrodynamic motion:

$$\left| \frac{1}{I}\frac{dI}{dt} \right|^{-1} \gg l/c_s ,$$

where $I(t)$ is the time-dependent current in a capillary of length l, through which flows a plasma whose sound velocity is c_s. For a typical $c_s \approx 1$ cm/μsec, one can see that this condition is obeyed in our case.

The model is based on the following assumptions.

(i) The plasma is optically thick and can be treated as a blackbody. This assumption does not necessarily contradict the fact that we observe spectral lines in the visible region, since the predicted temperatures are above 1 eV and as a result the thermal radiation is expected to be mainly in the uv region.

(ii) The plasma is characterized by a mass density and temperature which do not change significantly along the tube.

(iii) The plasma originates from polyethylene molecules $(CH_2)_n$ which are completely dissociated into partially ionized hydrogen and carbon atoms.

(iv) The heat exchange between the plasma and the walls is dominated by radiation.

It can be shown[1] that the discharge can be divided radially into two regions. The central region contains a nearly homogeneous plasma with temperature T and mass density ρ while the thin peripheral region separating the plasma from the walls exhibits sharp temperature and density gradients. The radial temperature gradient is negative while the density gradient is positive. Therefore energy is radiated from the plasma to the walls and returned by an appropriate ablated mass flow toward the central region.

Under steady-state conditions, the plasma characteristics can be obtained from energy- and mass-conservation considerations. First, the power radiated to the wall $S_{\rm rad}$ is set equal to the power returned to the plasma as internal energy of the ablated mass $S_{\rm abl}$. Radiation losses from the outer region are neglected, based on the sharp gradient assumption. The vaporization energy of polyethylene and the kinetic energy of the ablated mass are shown to be small and are neglected too.[1] The energy balance for the whole system gives

$$S_\Omega + S_{\rm abl} = S_{\rm rad} + S_{\rm jet} ,$$

where S_Ω is the Ohmic heating term while $S_{\rm jet}$ represents the energy of the plasma jet flowing through the open electrode. Since mass is conserved, $S_{\rm jet} = S_{\rm abl} = \gamma \varepsilon \dot{m}$, where $\dot{m}$ is the mass ablation rate of the capillary walls, ε is the specific internal energy of the plasma, and γ is the adiabatic coefficient defined through $\gamma - 1 = P/\rho\varepsilon$, P and ρ being the pressure and density of the plasma. Thus we get

$$S_\Omega = S_{\rm rad} = S_{\rm abl} = S_{\rm jet} = S .$$

The capillary resistance is given by

$$R = \beta R_s .$$

R_s is Spitzer's resistance for fully ionized plasma:[9]

$$R_s = 0.17 \left[\frac{l}{a^2} \right] (\ln\Lambda)/T^{3/2} ,$$

where l is the capillary length in cm and a is the capillary radius in mm, $\ln\Lambda$ is the Coulomb logarithm,[9] and T is the temperature in eV. β takes account of the presence of neutrals in the plasma:[1]

$$\beta = 1 + \frac{\nu_{e0}}{\nu_{ei}} = 1 + 5.6\times 10^{-2} \frac{T^2}{\ln\Lambda} \frac{N_0}{N_i} ,$$

where ν_{e0} and ν_{ei} are the electron-neutral and the electron-ion collision frequencies, and N_0 and N_i are the neutral and ion densities, respectively.

Spitzer's resistance together with the energy balance equations yield the expressions for the capillary resistance (in Ω) and temperature (in eV) in terms of the current (in kA):

$$R = 0.22 \frac{\beta^{8/11} l}{a^{13/11} I^{6/11}} ,$$

$$T = 1.35 \frac{\beta^{2/11} I^{4/11}}{a^{6/11}} .$$

The total power is obtained from the relation $S = I^2 R$, and the mass ablation rate from $\dot{m} = S/\gamma\varepsilon$. The plasma density is given by

$$\rho = \frac{\dot{m}}{\pi a^2 u_{\rm jet}} ,$$

where $u_{\rm jet}$ is the flow velocity of the plasma jet at the open electrode. Since the outer pressure vanishes, we take $u_{\rm jet} \approx c_s$. Based on some thermodynamic identities,[10] the plasma sound velocity can be written as

$$c_s^2 = \left[\frac{\partial P}{\partial \rho} \right]_T + \frac{T}{\rho^2} \frac{\left[\frac{\partial P}{\partial T} \right]_\rho^2}{\left[\frac{\partial \varepsilon}{\partial T} \right]_\rho} .$$

The plasma internal energy $\varepsilon(\rho, T)$ and the pressure $P(\rho, T)$ are calculated from the SESAME equation-of-state tables.[2] From the SESAME FORTRAN library, the rational function method is used to perform two-dimensional interpolation and calculation of first derivatives of the thermodynamic variables.

The neutral, ion, and electron densities are related through Saha equations:

$$\frac{N_{\rm H^+} N_e}{N_{\rm H}} = \frac{Z_{\rm H^+}}{Z_{\rm H}} 2 \left[\frac{2\pi m_e}{h^2} \right]^{3/2} T^{3/2} e^{-(E_I - \Delta E)/T} ,$$

where N_e, $N_{\rm H^+}$, and $N_{\rm H}$ are the number densities of electrons, hydrogen ions, and atoms, respectively. E_I is the ionization energy from the ground state while ΔE is the change in this energy which reflects the energy released on immersing an electron-ion pair in the plasma.[4] $Z_{\rm H^+}$

and Z_H are the partition functions of the species, and, as a first approximation[1] their ratio is taken close to 1. A similar equation relates the densities of carbon ions, carbon atoms, and electrons. Since only first ionization is considered, $E_I(H)=13.6$ eV and $E_I(C)=11.26$ eV.

Together with the equations for charge and mass conservation, a nonlinear system of equations is obtained which is reduced to a polynomial in the electron density. Thus the behavior of the capillary plasma at quasi-steady-state is described by a set of coupled algebraic equations which are solved self-consistently by numerical computation.

[1]A. Loeb and Z. Kaplan, IEEE Trans. Magn. **25**, 342 (1989).

[2]*T-4 Handbook of Material Properties Data Bases, Vol. Ic: Equations of State,* edited by K. S. Holian (Los Alamos National Laboratory, Los Alamos, 1984).

[3]H. R. Griem, *Spectral Line Broadening by Plasma* (Academic, New York, 1974).

[4]H. R. Griem, *Plasma Spectroscopy* (McGraw-Hill, New York, 1964).

[5]D. H. Oza, R. L. Greene, and D. E. Keller, Phys. Rev. A **37**, 531 (1988).

[6]W. Hermann, U. Kogelschatz, K. Ragaller, and E. Schade, J. Phys. D **7**, 607 (1974).

[7]L. Niemeyer, IEEE Trans. Power Appar. Syst. **PAS-97**, 950 (1978).

[8]E. Z. Ibrahim, J. Phys. D **13**, 2045 (1980).

[9]L. Spitzer, *Physics of Fully Ionized Gases* (Interscience, New York, 1956).

[10]S. Eliezer, A. Ghatak, and H. Hora, *An Introduction to Equations of State Theory and Applications* (Cambridge University Press, Cambridge, England, 1986), Chap. 2.